Separation Science and Technology
Publication details, including instructions for authors and subscription information:
http://www.informaworld.com/smpp/title~content=t713708471

Particle Filtration for Determination of Pore Size Characteristics of Microporous Membranes: Applicability to Plasma Separation Membranes

Akinori Sueoka[a]; Paul S. Malchesky[a]; Yukihiko Nose[a]
[a] DEPARTMENT OF ARTIFICIAL, ORGANS CLEVELAND CLINIC FOUNDATION, CLEVELAND, OHIO

To cite this Article Sueoka, Akinori , Malchesky, Paul S. and Nose, Yukihiko(1983) 'Particle Filtration for Determination of Pore Size Characteristics of Microporous Membranes: Applicability to Plasma Separation Membranes', Separation Science and Technology, 18: 6, 571 — 584
To link to this Article: DOI: 10.1080/01496398308060295
URL: http://dx.doi.org/10.1080/01496398308060295

SEPARATION SCIENCE AND TECHNOLOGY, 18(6), pp. 571-584, 1983

Particle Filtration for Determination of Pore Size Characteristics of Microporous Membranes: Applicability to Plasma Separation Membranes

AKINORI SUEOKA, PAUL S. MALCHESKY, and YUKIHIKO NOSE

DEPARTMENT OF ARTIFICIAL ORGANS
CLEVELAND CLINIC FOUNDATION
CLEVELAND, OHIO 44106

Abstract

Pore characteristics of microporous membranes were studied by filtration with aqueous solutions containing spherical particles of uniform diameter. The rejection values for four types of plasma separation membranes of microporous structure show good linearity to particle size with high correlation on log-normal probability coordinates. The mean pore size of 94 to 866 Å and standard deviation of 1.51 to 2.13 were obtained for these membranes. Such membranes have mean pore sizes of about one order of magnitude larger than that for synthetic dialysis and hemofiltration membranes in addition to having wider pore distributions. The mean pore sizes obtained by this study relate closely to sieving properties of macromolecules from blood.

INTRODUCTION

Microporous membranes of varying styles, film and hollow fiber, have been used for various filtration applications (*1, 2*). such membranes have been applied clinically for the on-line separation from whole blood (*3*) for source plasma collection and therapeutic treatments as plasma sorbent treatment and cryofiltration. The microstructure characteristics of the membrane are critical for achieving adequate filtration and sieving of plasma solutes. Therefore, it is highly desirable to evaluate the pore characteristics of these membranes. The evaluation of pore characteristics for membranes, such as those predominantly employed for plasma separation, is difficult due

 0149-6395/83/1806-0571$3.50/0

to their complicated structure. No generalized method for their evaluation has been proposed to date.

This study was intended to evaluate the pore characteristics of microporous membranes by filtration with uniform and known size particles.

METHODS OF PORE SIZE EVALUATION

Several evaluation methods are applied in the determination of pore size for microporous membranes; namely, the bubble point method, mercury intrusion, solvent permeability, observation by an electron microscope, and filtration of particles.

For the bubble point (*4*) and mercury intrusion methods (*5*), the membrane pore diameter is calculated by

$$d = 2\sigma \cos \theta / P \tag{1}$$

where d is the pore diameter of the membrane, σ is the surface tension (water/air in bubble point and mercury/air in mercury intrusion method), θ is the contact angle (water/membrane and mercury/membrane), and P is the applied pressure. The bubble point method is used mainly for quality control and evaluation of the maximum pore size. The limitations of this method are that only the maximum pore size is given, different values are given between the calculated pore size from Eq. (1) and that obtained by other methods, and high pressures of above 5 atm are needed for the membranes with pore sizes of less than 0.1 μm. The mercury intrusion method gives the mean pore size, pore distribution, and pore volume. The limitation of this method is that pressures of 10 to 100 atm are needed. Both of these methods require pressure in excess of those normally encountered in normal operation of membrane plasma separation (pressure less than 0.5 atm).

Pore diameter is also obtained by the solvent (water) permeability method (*6*) using the Hagen-Poiseulle equation under conditions of laminar flow:

$$d = \left(\frac{128 \eta L J}{n \pi P} \right)^{1/4} \tag{2}$$

where η is the viscosity of the solvent, L is the length of the pore, n is the number of pores, and J is the flux. This method is based on the assumption that the pore is a straight-through cylindrical shape, and therefore cannot be strictly applied to tortuous pore structures such as these predominantly found in membranes for plasma separation.

Observation by electron microscope is helpful in that it directly gives details of the whole pore structure and pore shape. However, electron microscopic observations are performed on discrete and minute samples which may or may not be representative of a production lot, and are limited in defining the pore size of complicated pore structures. Further practical limitations of observation are reached for pore sizes smaller than 0.1 μm.

Filtration methods are based on the measurement of rejection or sieving for known sizes of particles or solutes. This method is primarily used for ultrafiltration membranes (*7*) with single solute solutions of varying molecular weight solutes. The pore size of the membrane is expressed in terms of the molecular weight cut off. For microporous membranes, the filtration of particles and bacteria are used. This method gives working information of filtration selectivity of a given membrane for a given liquid. In this method it is important to select uniform sized particles over a wide range of sieving corresponding to the membrane under investigation. The limitation of this method is that rejection (1 − sieving) or sieving values are variable depending upon the operation conditions which may cause deposition of particles on the membrane.

Kamide et al. (*8*) reported the pore size evaluations for microporous track etched (straight-through pores) membranes using various techniques including bubble point, mercury intrusion, fluid permeability, gas permeability, and electron microscopy. They concluded that pore size estimation is independent of the measuring method used for the track-etched membranes of Nuclepore, but size estimation is highly variable for the tortuous-type membranes. Most descriptions of membranes and evaluations involve a multiplicity of methods.

EXPERIMENTAL METHODS AND MATERIALS

Five styles of commercial plasma separation membrane modules of large surface area (0.32–0.80 m^2) and four styles of small surface area modules fabricated in the laboratory (0.04–0.06 m^2) were evaluated as shown in Table 1. Two membrane types were studied: polyvinyl alcohol (*9*) (Kuraray Co., Osaka, Japan) styles S, M, and 400; and cellulose acetate (*10*) (Asahi Medical Co., Tokyo, Japan) styles PF-01 and PF-02. Small surface area modules containing 150 to 400 fibers mounted in M-type module were fabricated using the commercial plasma separator membranes and epoxy resin as the potting material.

Seven sizes of particle solutions of uniform size made of styrene-butadiene latex and colloidal silica and suspended in water were selected and used in this study as listed in Table 2. The filtration of particle solutions was carried

TABLE I
Characterization of Filter

	Membrane					Module				
Filter	Membrane type	Manufacturer	Inside diameter (μm)	Wall thickness (μm)	Material	Module type	Manufacturer	Length of fiber (cm)	Number of fibers	Surface area (m^2)
PVA-SA	S	Kuraray	330	125	PVA[a]	A	Kuraray	29	2100	0.63
PVA-SM						M	CCF[c]	20	300	0.06
PVA-MA	M	Kuraray	400	200	PVA	A	Kuraray	29	1100	0.40
PVA-MM						M	CCF	20	150	0.04
PVA-400B	400	Kuraray	400	200	PVA	B	Kuraray	23	1100	0.32
PF-01	PF-01	Asahi	370	160	CA[b]	Plasmaflo	Asahi	20	3400	0.80
PF-01M						M	CCF	12	300	0.04
PF-02	PF-02	Asahi	330	75	CA	Hi-05	Asahi	17	3400	0.60
PF-02M						M	CCF	10	400	0.04

[a]PVA = Polyvinyl alcohol.
[b]CA = Cellulose acetate.
[c]Laboratory produced.

TABLE 2
Properties of Particle

Particle	Manufacturer	Particle size (Å)	Material	Initial particle concentration (%)
SBR-636	Dow Chemical, USA	2000	Stylene-butadiene Latex	50
Snowtex-20L	Nissan Chemical, Japan	450 (400–500)	Colloidal silica	20
30		150 (100–200)		30
Ludox-TM	Dupont Chemical, USA	235 (220–250)	Colloidal silica	50
HS-30		135 (130–140)		30
SM		75 (70–80)		30
Cataloid-SI30	Shokubai Kasei, Japan	120 (100–140)	Colloidal silica	30

out by utilizing a closed filtrate circuit as shown in Fig. 1 which is similar to that used in plasma separation studies (*11*). The temperature was maintained at 25°C.

In order to select the most optimum testing conditions, preliminary tests were carried out using PVA-400B type units by (a) varying particle concentrations from 0.1 to 5% at a constant flow rate (Q_i) of 100 mL/min (wall shear rate, $\bar{\gamma}_w$, of 200 s^{-1}) and filtrate flow rate (Q_F) of 5 mL/min, (b) varying Q_F from 5 to 20 mL/min at constant Q_i of 100 mL/min and constant inlet particle concentration of 1%, and (c) varying Q_i from 100 to 320 mL/min ($\bar{\gamma}_w$ = 190 to 600 s^{-1}) at constant Q_F of 10 mL/min and constant inlet particle concentration of 1%. $\bar{\gamma}_w$ was calculated from

$$\bar{\gamma}_w = (2Q_i - Q_F)/30N\pi r^3 \tag{3}$$

where N is the number of fibers and r is the radius of fiber.

The transmembrane pressure (P) was monitored and the rejection of particles was measured during the study. Particle concentration was measured by weight determination of the solids following drying. The particle rejection was calculated as

$$\text{Rejection (\%)} = \left(1 - \frac{\text{particle wt\% in filtrate}}{\text{particle wt\% in inlet solution}}\right) \times 100 \tag{4}$$

From the results of the preliminary studies, the standard operating conditions were selected as $\bar{\gamma}_w$ of 200 s^{-1} (shear rate typically used for clinical operation (*3*)), Q_F at one-tenth of Q_i, and a particle concentration at

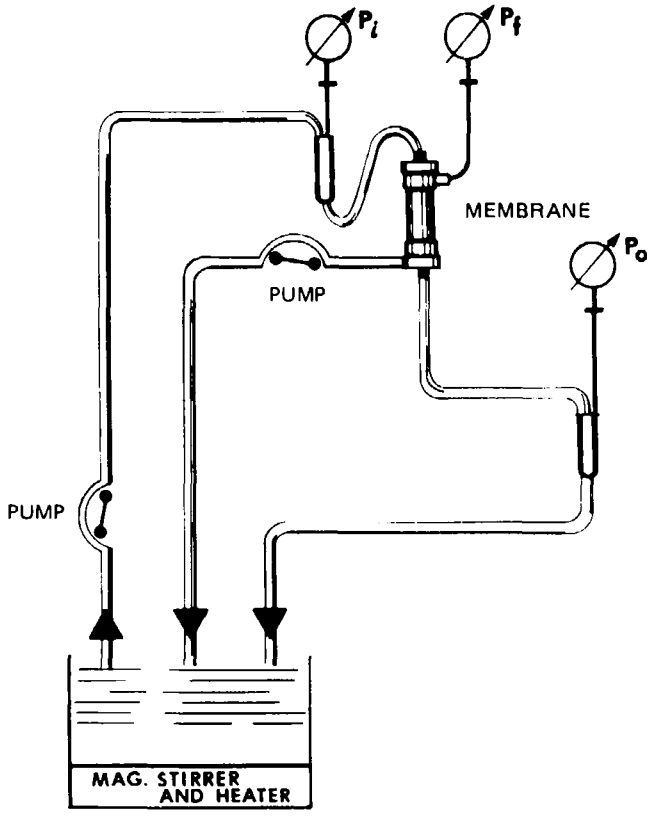

FIG. 1. Test circuit.

1%. Q_i is calculated from Eq. (3). The rejection value was calculated by averaging the rejection results during the first 10 to 60 min of filtration as

$$\text{Rejection} = \left(1 - \frac{\Sigma C_F Q_F \Delta t}{\Sigma C_B Q_F \Delta t}\right) \times 100 \tag{5}$$

where C_F is the particle concentration of the filtrate, C_B is the particle concentration of the inlet solution, and Δt is a time interval between measurements. The initial filtrate was discarded since appreciable dilution of the filtrate occurs in the early minutes due to water extraction from the pores.

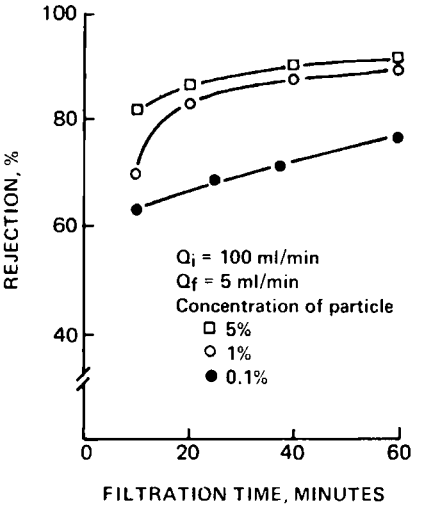

FIG. 2. Rejection versus perfusion time at varying concentrations of 2000 Å latex particles. The inlet flow rate was 100 mL/min. The filtrate flow rate was 5 mL/min. The filter module was the PVA-400B.

RESULTS AND DISCUSSION

Figures 2–4 give the results of the preliminary tests using PVA-400B units and 2000 Å particle solutions. The higher the particle concentration for the range of 0.1 to 5%, the higher the rejection, as shown in Fig. 2. In general, a Q_F between 5 and 20 mL/min has little effect on rejection (Fig. 3). The higher the shear rate, the lower the rejection. These results are related to the bulk concentration and wall shear rate effects, and qualitatively agree with the results of blood filtration studies carried out; that is, plasma filtration increases with wall shear rate and the amount of filtrate decreases in proportion to the inlet particle concentration (blood cell volume). It is noted from these results that there is an effect of filtration time; for these low concentrations of particles in solution (for whole blood the normal particle concentration is 40 to 50%), rejection increases with time before a steady-state value of rejection is achieved. This effect is believed related to a build up of particles on the membrane wall and the gradual and partial or total plugging of the smaller pores. This time dependency is not noteworthy in studies with blood of normal composition, perhaps due to its high particle concentration. Quantitation of the amount and type of deposition occurring with whole blood is difficult and probably membrane-type dependent.

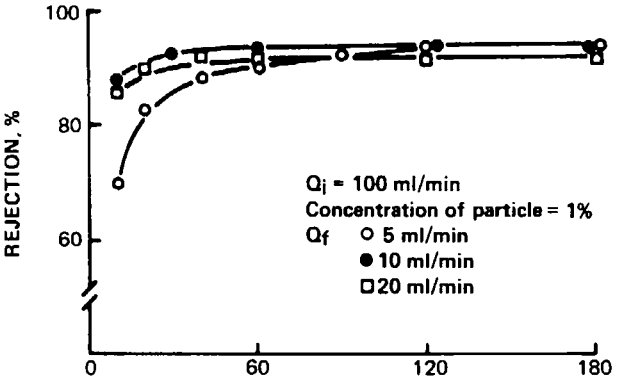

FIG. 3. Rejection versus perfusion time at varying filtrate fow rates. A 1% concentration of 2000 Å latex particles was employed. The inlet flow rate was 100 mL/min. The filter module was the PVA-400B.

Rejection values for the seven sizes of particles under the standard operating conditions are listed in Table 3 for four of the types of membrane studied. Rejection values increase with increasing particle size. The rejection for particles as a function of particle size is shown in Fig. 5 for various membrane types. The results indicate that the PVA-S type membrane has the largest pore size and PF-01 the smallest pore size of the membrane studied. PVA-M and PF-02 type membranes show similar rejection curves. Rejection curves for each membrane are described as S-shaped on rejection versus log particle size plots.

Rejection curves describing the S-shape suggest that the application of the log-normal distribution function as reported by Michaels (*12*) is acceptable for the relationship between rejection and particle size. If rejection correlates with particle size by the log-normal probability function, this relationship is expressed as

$$\mathrm{Re} = \mathrm{erf}\,(z) \tag{6}$$

where

$$\mathrm{erf} = \frac{1}{\sqrt{2}} \int_{-\infty}^{u} \exp\left(\frac{-y^2}{2}\right) dy$$

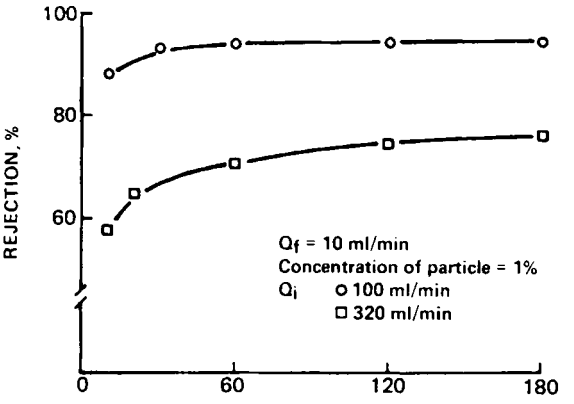

FIG. 4. Rejection versus perfusion time at varying inlet flow rates. A 1% concentration of 2000 Å latex particles was emplyed. The filtrate flow rate was 10 mL/min. The filter module was the PVA-400B.

TABLE 3
Rejection Data for Varying Membrane

Membrane type	Particle size (Å)	Rejection (%)	z^a
PVA-S	2000	82.9	0.950
	450	30.0	−0.525
	235	4.9	−1.655
	150	0.5	−2.575
PVA-M	450	95.0	1.645
	235	70.5	0.539
	135	35.4	−0.375
	120	28.3	−0.574
	75	17.6	−0.931
PF-01	235	99.0	2.320
	135	77.6	0.759
	120	67.8	0.461
	75	34.0	−0.414
PF-02	450	97.6	1.975
	235	86.6	1.108
	135	11.7	−1.190
	120	11.5	−1.200
	75	7.6	−1.435

[a]Normal equivalent deviate.

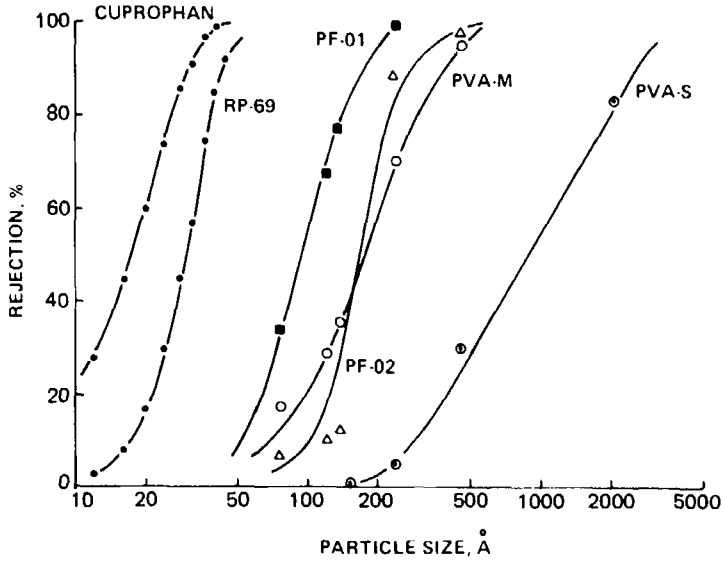

FIG. 5. Rejection versus particle size for varying synthetic membranes. Cuprophan and RP-69 data taken from Michaels (*12*).

$$z = \frac{\log (a/\bar{a})}{\log \sigma_a} \tag{7}$$

Re = rejection, a = particle size, $\bar{a}$ = mean particle size (for which Re = 50%), and σ_a = the geometric standard deviation about $\bar{a}$. From Eq. (6) and (7), the linear relationship derived on log-probability coordinate is

$$f(\mathrm{Re}) = A + B(\log a) \tag{8}$$

As z values are used for normal equivalent deviate ($f(\mathrm{Re}) = 0$ at Re = 50%),

$$f(\mathrm{Re}) = A + B(\log a) = z \tag{9}$$

Values of z at a given Re are obtained from tables of statistics (normal equivalent deviate of cumulative frequency). For example, z is 0 at Re = 50%, −1 at Re = 15.8%, and 1 at Re = 84.2%. Equation (9) can be analyzed using experimental data of a and z values. A and B are the intercept and slope, respectively. At Re = 50% ($z = 0$), $\bar{a}$ is determined from Eq. (9). σ_a is determined from the ratio of a at Re = 84.1% ($z = 1$) and $\bar{a}$. $\bar{a}$ is

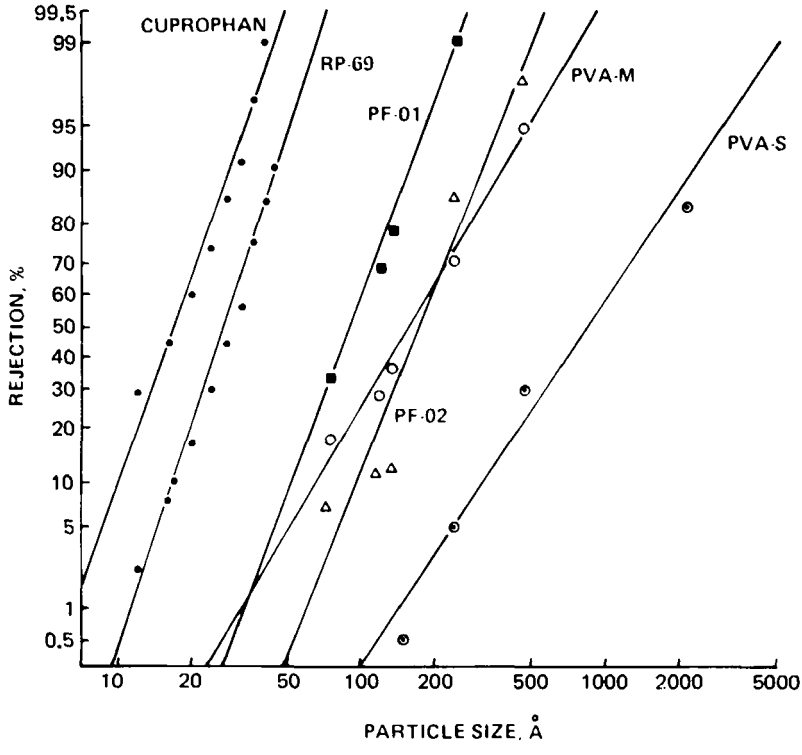

FIG. 6. Rejection versus particle size for varying synthetic membranes on log-normal probability coordinates. Cuprophan and RP-69 data taken from Michaels (*12*).

defined as "the mean pore size" of the membrane. σ_a is the measure of sharpness of the pore distribution.

Table 3 lists z values for the rejection data obtained by this study. The data for rejection as a function of particle size are plotted for four membrane types in Fig. 6 on log-normal probability coordinates. Good linearity with high correlation is seen for each membrane. $\bar{a}$, σ_a, A, B, and the correlation coefficients for the data fit of each membrane are listed in Table 4. The S-shape rejection curves of Fig. 5 are therefore well characterized by the log-normal probability function. This analytical method provides a reasonable guideline for the evaluation of membrane pore size for plasma separation membranes. A mean pore size ($\bar{a}$) of 866 Å and σ_a of 2.13 were obtained for the PVA-S type, 160 Å and 1.95 for the PVA-M type, 94 Å and 1.51 for the PF-01 type, and 178 Å and 1.58 for the PF-02 type membranes. σ_a relates to B (slope); decreasing σ_a results in increasing B. The range of σ_a falls between

TABLE 4
Mean Pore Size and Standard Deviation for Varying Membranes

	PVA-S	PVA-M	PF-01	PF-02
Number of Data Points	4	5	4	5
A	−8.949	−7.581	−10.947	−11.309
B	3.046	3.440	5.548	5.025
Mean pore size, $\bar{a}$ (Å)	866	160	94	178
Standard Deviation, σ_a	2.13	1.95	1.51	1.58
Correlation coefficient	0.985	0.990	0.992	0.953

1.51 and 2.13. Lower values of σ_a imply a narrower pore size distribution. It is seen that the sharpness of pore distribution for the PF-01 and PF-02 type membranes is higher than for the PVA-S and M type membranes. To compare the pore size and pore distributions of the plasma separation membranes to membranes used in dialysis and hemofiltration, data taken from Green et al. (*13*) and Michaels (*12*) on dialysis and hemofiltration membranes are plotted together with the data obtained in this study in Fig. 5 as rejection versus log particle size and in Fig. 6 as probability of rejection versus log particle size. Michaels (*12*) reported $\bar{a}$ and σ_a values for synthetic dialysis and ultrafiltration membranes of 17 to 28 Å and 1.33 to 1.66 for σ_a, respectively. Plasma separation membranes have mean pore sizes about one order of magnitude larger than that for dialysis and hemofiltration membranes in addition to having wider pore distributions.

Currently, the PVA-S type (PVA-SA module) and PF-02 type (Plasmaflo Hi-05) membranes are being used clinically as plasma separators, and PVA-M (PVA-MN) and PF-01 (Plasmaflo) for secondary filters in cryofiltration. Sieving coefficients for the PVA-SA and Plasmaflo Hi-05 modules are shown in Table 5 for a chronic cholestatic patient treated by plasma

TABLE 5
Sieving Coefficients for PVA-SA and Plasmaflo Hi-05 in Plasma Exchange[a]

	PVA-SA	Plasmaflo Hi-05
Number of treatments	8	10
Concentration of total cholesterol, mg/dL	522 ± 57	605 ± 113
Sieving coefficient:		
Albumin	0.97 + 0.02	0.91 + 0.04
Total protein	0.97 ± 0.03	0.86 ± 0.05
Total cholesterol	0.96 ± 0.03	0.46 ± 0.11

[a]Patient: chronic cholestatic. Filtration condition: Blood flow rate = 100–120 mL/min, plasma flow rate = 20–30 mL/min, 2 L plasma exchange with 3.7% albumin.

TABLE 6
Sieving Coefficients for PVA-MN and Plasmaflo (PF-01) in *In Vitro* Cryofiltration[a]

Sieving coefficient	PVA-MN	Plasmaflo
Total protein	0.86	0.83
Albumin	0.94	0.84
Total cholesterol	0.82	0.64
IgG	0.87	0.81
IgM	0.87	0.53

[a] Plasma: Normal human plasma. Filtration conditions: Temperature = 4°C, transmembrane pressure = 10–16mmHg.

exchange. The PVA-SA module gives higher sieving compared to the Hi-05, especially for total cholesterol. The sieving properties for the PVA-MN and Plasmaflo in *in vitro* cryofiltration studies using normal human plasma are shown in Table 6. In general, the PVA-MN module has higher sieving, especially for the higher molecular weight solutes. These results indicate that the differences in sieving seen for membrane types relate closely to the membrane pore size obtained from this study.

Recently, other types of membrane plasma separators (*14*) with varying polymer types as cellulose acetate, polyvinyl alcohol, polymethyl methacrylate, polyethylene, polypropylene, polysulfone, and polycarbonate have been developed. The evaluation of pore characteristics as described in this study can be especially useful in the analysis of these membranes for clinical filtration applications.

REFERENCES

1. M. C. Porter, in *World Filtration Congress III*, Vol. II, 1982, p. 451.
2. P. S. Malchesky and Y. Nose, *Ibid.*, Vol. II, 1982, p. 649.
3. P. S. Malchesky, Y. Asanuma, J. W. Smith, K. Kayashima, I. Zawicki, W. Werynski, M. Blumenstein, and Y. Nose, *Trans. Am. Soc. Artif. Intern. Organs, 27*, 439 (1981).
4. M. C. Porter, "Membrane Filtration," in *Handbook of Separation Techniques for Chemical Engineers* (P. A. Schweitzer, ed.), McGraw-Hill, New York, 1979, Section 2, p. 89.
5. R. E. Kesting, in *Synthetic Polymer Membranes* (R. E. Kesting, ed.), McGraw-Hill, New York, 1972, p. 31.
6. R. E. Kesting, in *Synthetic Polymer Membranes* (R. E. Kesting, ed.), McGraw-Hill, New York, 1972, p. 32.
7. R. W. Baker and H. Strathmann, *J. Appl. Polym. Sci., 14*, 1197 (1970).
8. K. Kamide and S. Manabe, in *Ultrafiltration Membranes and Applications* (A. R. Cooper, ed.), Plenum, New York, 1979, p. 173.

9. A. Sueoka, J. Wojcicki, P. S. Malchesky, and Y. Nose, in *Plasmapheresis: Therapeutic Applications and New Techniques* (Y. Nose, P. S. Malchesky, J. W. Smith, and R. S. Krakauer, eds.), Raven Press, 1983.
10. P. S. Malchesky, A. Werynski, Y. Asanuma, I. Zawicki, J. W. Smith, H. Gurland, and Y. Nose, *Artif. Organs, 5*(Suppl), 113 (1981).
11. A. Werynski, P. S. Malchesky, A. Sueoka, Y. Asanuma, J. W. Smith, K. Kayashima, E. Herpy, H. Sato, and Y. Nose, *Trans. Am. Soc. Artif. Intern. Organs, 27*, 539 (1981).
12. A. S. Michaels, *Sep. Sci. Technol., 15*(6), 1305 (1980).
13. D. M. Green, G. D. Antwiter, J. W. Moncrief, J. F. Decherd, and R. P. Popvich, *Trans. Am. Soc. Artif. Intern. Organs, 22*, 627 (1976).
14. H. J. Gurland, W. Samtleben, and M. Blumenstein, *Life Support Syst., 1*, 61 (1983).

Received by editor December 9, 1982
Revised January 31, 1983